

A Millimeter-Wave GaN MMIC Front End Module with 5G NR Performance Verification

Ji-Hye Hwang¹ · Jiho Lee¹ · Ki-Jin Kim² · Han Lim Lee^{1,*}

Abstract

This paper proposes a millimeter-wave (mmWave) 5G front end module (FEM) based on multiple gallium nitride (GaN) monolithic microwave integrated circuits (MMICs) with 5G new radio (NR) performance verification. The proposed structure is configured by a wide band GaN single-pole double-throw (SPDT) switch MMIC, a GaN low-noise amplifier (LNA) MMIC, and a GaN power amplifier (PA) MMIC with the target operation band from 26.5 GHz to 29.5 GHz. The LNA and PA MMICs are designed with 150 nm GaN/SiC technology, and the SPDT MMIC is designed with 100 nm GaN/Si. The LNA MMIC shows the measured noise figure less than or equal to 2.52 dB within the operation band. The PA MMIC is based on a two-stage configuration and shows about 35 dBm measured saturated power with power-added efficiency better than 34% within the operation band. Also, the SPDT MMIC is based on an artificial transmission line configuration for wideband performance and shows that the measured insertion loss is less than 1.6 dB, and the measured isolation is higher than 25 dB within the operation band. Furthermore, all MMICs are integrated within a single carrier as an FEM and successfully verified by 5G NR test signals.

Key Words: FEM MMIC, GaN/Si MMIC, GaN/SiC MMIC, mmWave LNA, mmWave PA, mmWave SPDT.

I. INTRODUCTION

With the increasing demand for high-capacity, high-throughput and low-latency communication, the practical deployment of millimeter-wave (mmWave) 5G is being intensively investigated to leverage the full potential of next-generation communications. Since the transmitter and receiver core architecture must undergo radical innovations in the mmWave spectrum, the unprecedented challenges in the wave transmission and propagation efficiency in the mmWave band must be thoroughly considered. To meet the required specifications of mmWave-5G applications, the conventional circuit fabrications with CMOS or GaAs technologies are no longer sufficient in

terms of both performance criteria and power efficiency. In particular, the critical limitation of a GaAs HEMT is its relatively low power density, resulting in unsatisfactory output power generation for high power request. Owing to the need for high-frequency high power amplifiers (PAs) and high-voltage devices in power electronics, the gallium nitride (GaN) technology has been rapidly growing with its capability in handling high power and continuous effort to reduce the fabrication cost.

Since the primary advantage of GaN HEMT technology is emphasized by its high-power capability, many mmWave GaN PA MMICs (monolithic microwave integrated circuits) on both silicon carbide (SiC) and silicon (Si) substrates have been previously reported [1–5]. Furthermore, with the emergence of the

Manuscript received March 2, 2022 ; Revised June 10, 2022 ; Accepted July 21, 2022. (ID No. 20220302-023f)

¹School of Electrical and Electronics Engineering, Chung-Ang University, Seoul, Korea.

²ICT Device/Packaging Research Center, Korea Electronics Technology Institute, Seongnam, Korea.

*Corresponding Author: Han Lim Lee (e-mail: hanlimlee@cau.ac.kr)

This is an Open-Access article distributed under the terms of the Creative Commons Attribution Non-Commercial License (<http://creativecommons.org/licenses/by-nc/4.0>) which permits unrestricted non-commercial use, distribution, and reproduction in any medium, provided the original work is properly cited.

© Copyright The Korean Institute of Electromagnetic Engineering and Science.

mmWave-5G market, high-performance and cost-effective multifunctional chips for both transmitter and receiver designs are in significant demand. Since GaN also provides good noise performance, GaN MMIC-based front end modules (FEMs) have been also proposed in different bands covering S-, C-, X-, and Ku-bands [6–10]. However, despite there being many individual GaN MMICs, there have been few existing studies on a complete Ka-band component including switch, PA, and LNA MMICs, as an integrated module. Moreover, there are few GaN MMIC FEMs with practical 5G new radio (NR) measurement and verification. Thus, in this paper, a mmWave FEM configured by a GaN/SiC PA, a GaN/SiC LNA, and a GaN/Si single-pole double-throw (SPDT) switch MMICs is designed for n257 band and verified with 5G NR test signals.

II. DESIGN AND ANALYSIS

Fig. 1 shows the proposed FEM based on a multichip configuration including PA, LNA, and SPDT switch MMICs within a package. The proposed FEM MMICs are designed with two commercially available process technologies: WINsemi 150 nm GaN/SiC for PA and LNA MMICs and OMMIC 100 nm GaN/Si for SPDT MMIC. The PA and LNA are designed with GaN/SiC to consider the power handling capability and efficiency, whereas SPDT is designed with GaN/Si to consider the cost-effectiveness. The process technology features are summarized in Table 1.

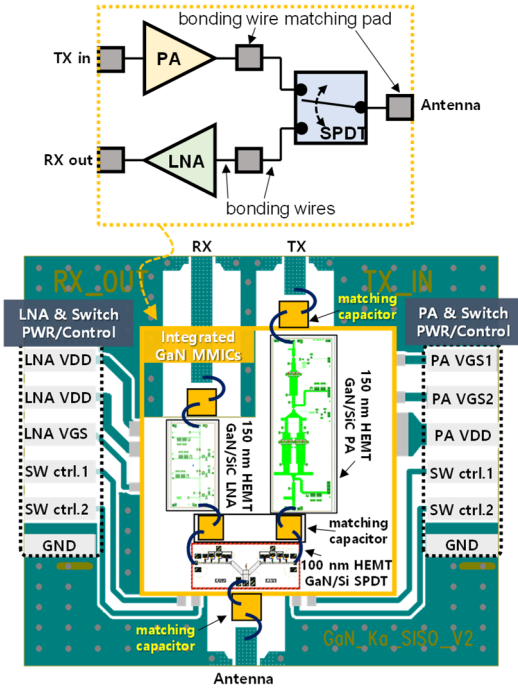


Fig. 1. Configuration of the proposed FEM based on GaN PA, LNA, and switch MMICs.

Table 1. Parameter summary of GaN HEMT processes

Parameter	HEMT process values	
	GaN/SiC	GaN/Si
Gate length (nm)	150	100
Substrate thickness (μm)	100	100
F_T (GHz)	34.5	110–180
Power density (W/mm)	4	4
Transconductance (mS/mm)	435	800
Noise figure @ 40 GHz (dB)	2	1.5
Max. drain current (A/mm)	0.985	1.2–1.7
Breakdown gate voltage (V)	120	36

1. GaN/SiC LNA and PA MMIC Design

Fig. 2 shows the DC characteristics of the different GaN/SiC HEMT sizes with a gate-source voltage step for 0.1 V from -2.5 V to 0 V. With the drain voltage of 20 V and gate biasing voltage of -1.2 V, the simulated power density of 480 μm HEMT is found as 4.81 W/mm. Also, with the drain voltage of 5 V and gate biasing voltage of -1.5 V, the simulated power density of 100 μm HEMT is determined as 1.25 W/mm. Next, both HEMT devices are simulated to determine the optimized impedances for the maximum output power of PA and noise figure (NF) of LNA from 26.5 GHz to 29.5 GHz. Fig. 3(a) shows the simulated source and load impedances of 480 μm HEMT as a PA unit cell with drain voltage of 20 V and gate voltage of -1.2 V on the Smith chart at 28 GHz. The simulated source and load impedances of $0.84 + j1.21 \Omega$ and $5.73 + j20.45 \Omega$, respectively are chosen to obtain the simulated maximum output power and PAE (power-added efficiency) of 32.4 dBm and 52.37%, respectively. In addition, Fig. 3(b) show the simulated source and load impedances of 100 μm HEMT as an LNA unit cell with drain voltage of 5V and gate voltage of -1.5 V on the Smith chart at 28 GHz. The simulated source and load impedances of $13.1 + j39.17 \Omega$ and $31.23 + j19.74 \Omega$ are chosen to obtain the simulated NF and available gain of 0.95 dB and

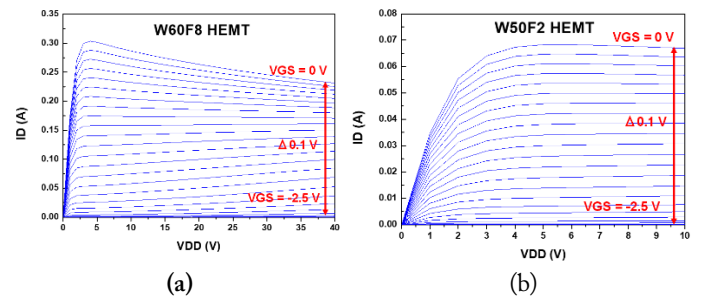


Fig. 2. DC characteristics of GaN/SiC HEMTs with (a) 480 μm and (b) 100 μm sizes.

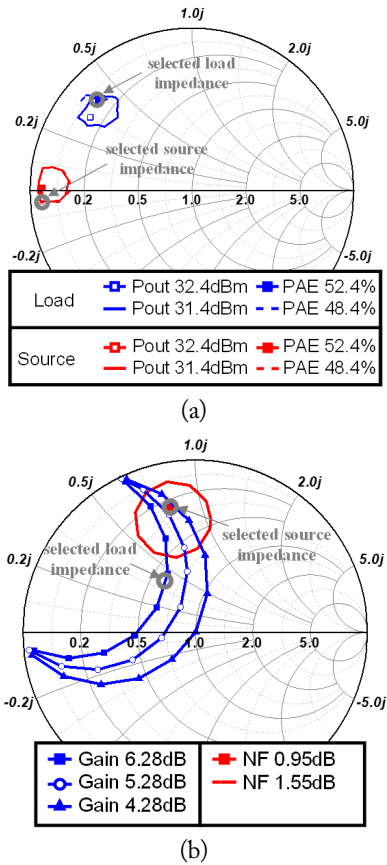


Fig. 3. Source and load pull simulated impedances of (a) 480 μm and (b) 100 μm GaN/SiC HEMTs.

6.28 dB, respectively. Based on the source and load pull simulations from 26.5 GHz and 29.5 GHz, the obtainable output power, gain, and PAE for the PA unit cell, and NF, gain, and PAE for the LNA unit cell are summarized in Table 2.

Using the selected 100 μm HEMT cells, a three-stage single-ended LNA is designed as shown in Fig. 4(a). The VDD and VGS for all stages are biased with 5 V and -1.5 V, respectively. Then, Fig. 4(b) shows the simulated S -parameters and NF of the designed LNA. The simulated minimum NF from 26.5 GHz to 29.5 GHz is about 1.62 dB, whereas the simulated minimum gain is about 20 dB. The gain variation is less than 1 dB within the operation band. In addition, Fig. 4(c) shows the simulated output P1dB from 26.5 GHz to 29.5 GHz. The minimum output P1dB of 10.5 dBm is observed at 29.5 GHz, while the

Table 2. Simulated parameter summary of the HEMT cells

	Freq. (GHz)	P_{out} (dBm)	Gain (dB)	PAE (%)
480 μm (PA unit cell)	26.5	32.4	16.47	52.39
	28.0	32.4	16.96	52.37
	29.5	32.4	16.67	47.45
100 μm (LNA unit cell)	26.5	0.91	6.34	20.34
	28.0	0.95	6.28	21.13
	29.5	1.07	6.16	21.83

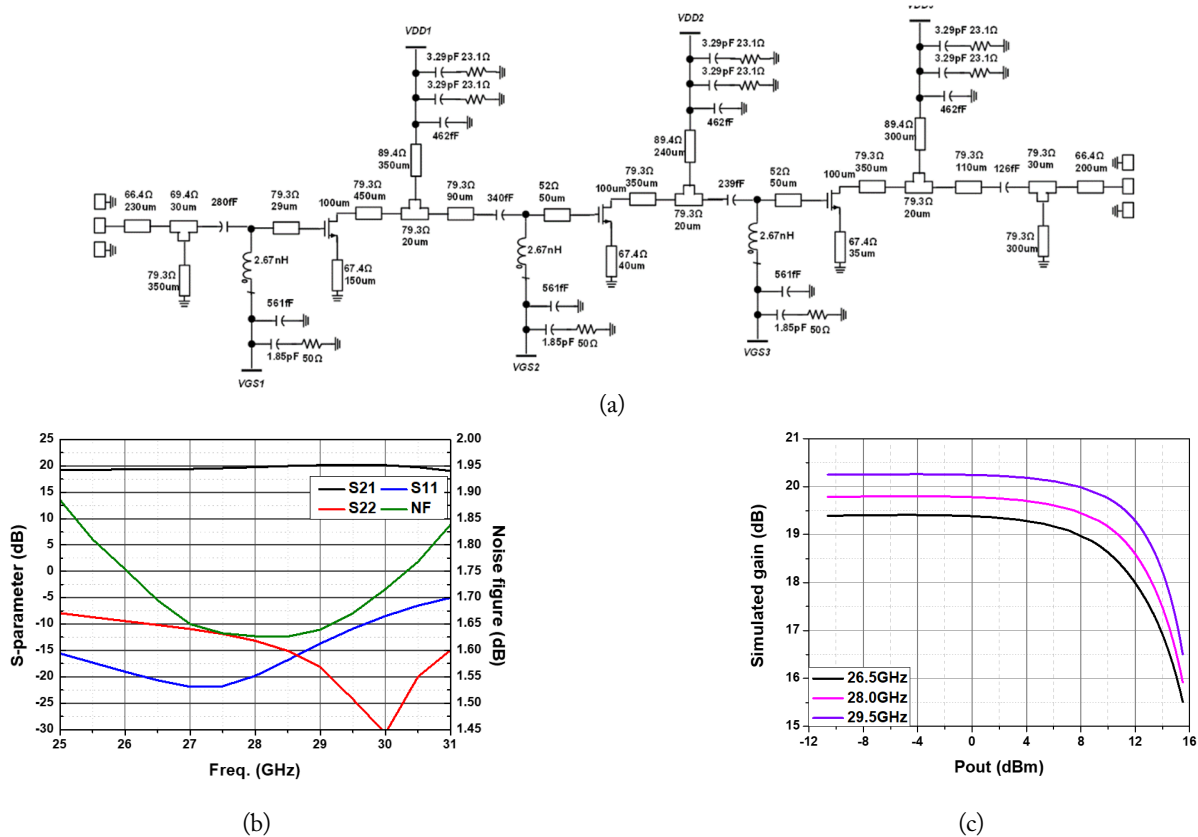


Fig. 4. GaN/SiC LNA MMIC with (a) a design schematic and simulated (b) S -parameters and NF, and (c) gain and output P1dB.

output P1dB variation within the operation band is less than 1.5 dB.

Next, a two-stage PA is designed with the selected $480\ \mu\text{m}$ HEMT devices, as shown in Fig. 5(a). The VDD and VGS in all stages are biased with 20 V and $-1.2\ \text{V}$, respectively. In the second stage, two HEMT cells are used for parallel power combining to achieve the simulated output power of 35.4 dBm. Fig. 5(b) and 5(c) show the simulated S -parameters and output P1dB from 26.5 GHz to 29.5 GHz. The maximum gain of the PA is about 22.4 dB at 26.5 GHz and the gain variation within the operation band is less than 2.5 dB. Also, the simulated minimum output P1dB of 27 dBm is observed at 29.5 GHz, while the P1dB variation within the operation band is less than 3 dB. Furthermore, Fig. 5(d) shows the simulated PAE of the PA, and the maximum PAE of 31.5% is observed at 28 GHz.

2. GaN/Si SPDT Switch MMIC Design

Fig. 6(a) and 6(b) show the typical switch characteristics of the GaN/Si HEMT device having the size of $50\ \mu\text{m}$. As the operation frequency reaches the mmWave band, the parasitic reactance and resistive loss of the HEMT device increase drastically, resulting in poor ON-and-OFF performance. Thus, to ensure wideband operation and high isolation between the ON and OFF states, an artificial transmission line-based SPDT switch is designed, as shown in Fig. 7(a). The simulated S -parameters are shown in Fig. 7(b). Here, the simulated insertion loss is always less than 0.97 dB, while the simulated isolation is

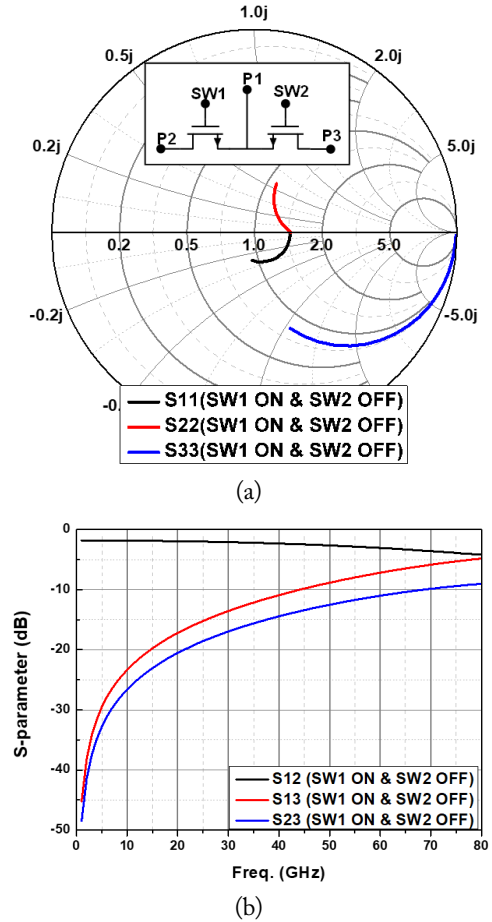


Fig. 6. GaN/Si HEMT switch characteristics with simulated (a) on and off state impedances and (b) S -parameters.

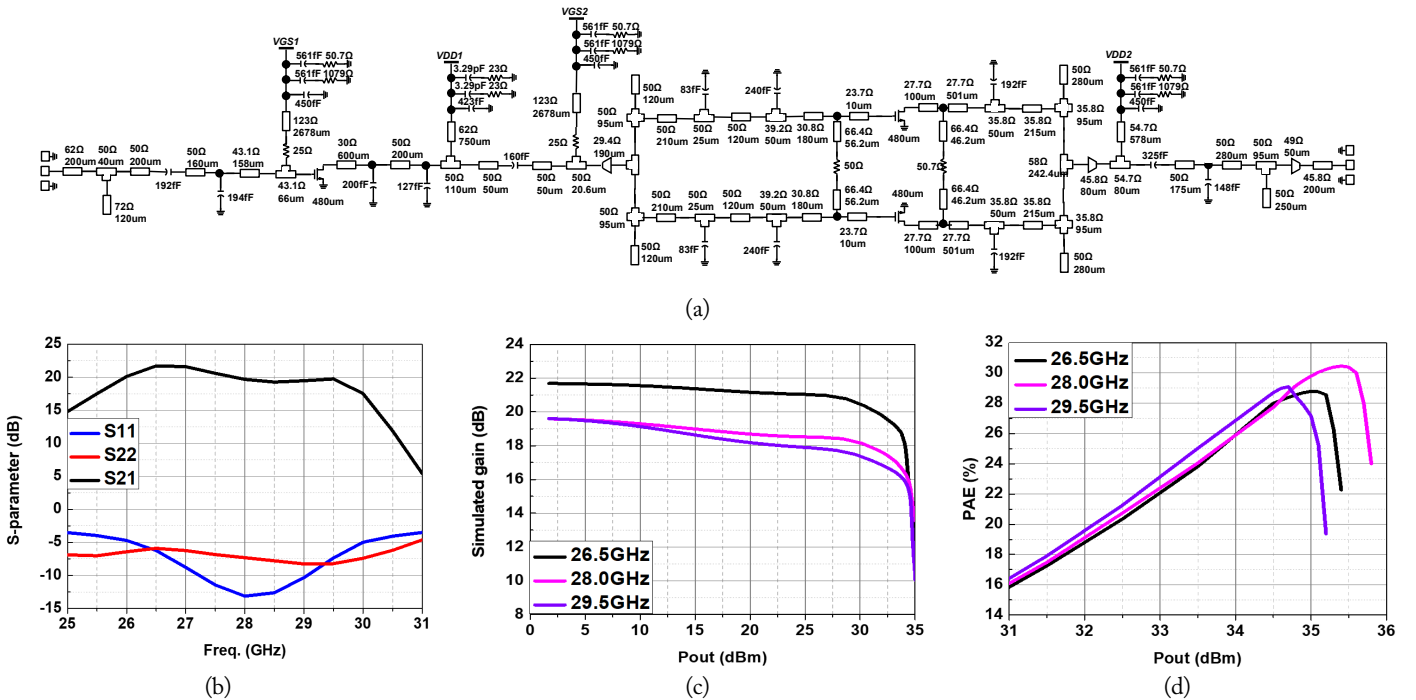


Fig. 5. GaN/SiC PA MMIC with (a) a design schematic and simulated (b) S -parameters, (c) output P1dB, and (d) PAE.

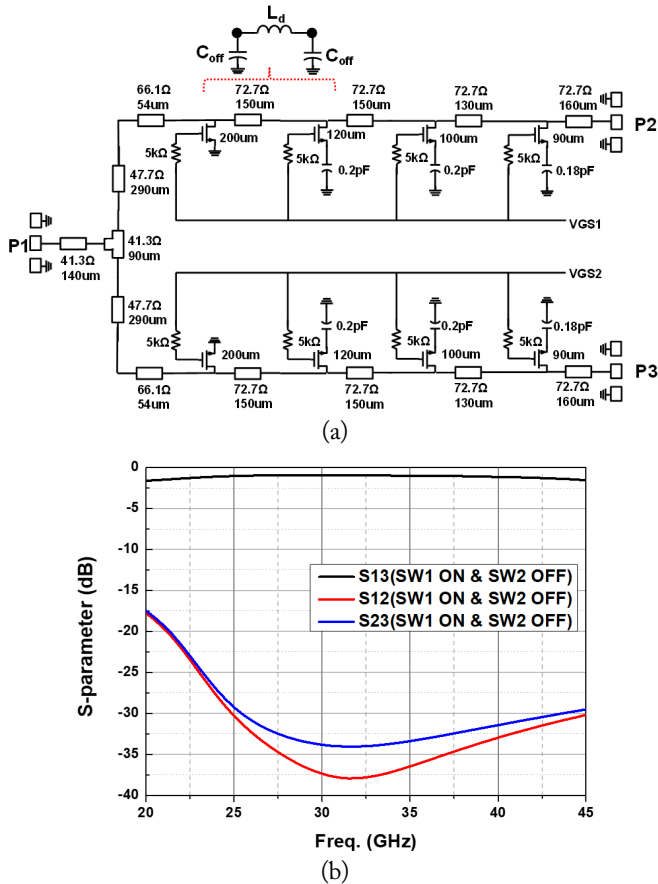


Fig. 7. GaN/Si HEMT-based SPDT MMIC with (a) schematic design and (b) simulated S -parameters.

always better than 31.5 dB within the selected operation bandwidth from 26.5 GHz to 29.5 GHz. Furthermore, the simulated input P1dB of the SPDT within the operation band is more than 40 dBm.

3. Bonding Wire with Transmission Line Matching

Since the proposed FEM is configured by multiple MMICs with bonding wire connections, the mismatch caused by the bonding wires must be considered. Thus, the printed circuit board (PCB) transmission lines with bonding wires are simulated as shown in Fig. 8(a). Specifically, the microstrip line with the bonding wire only is compared to the microstrip line with the bonding wire compensated by a matching pad. In the simulation, a Taconic TLY-5 substrate with a relative permittivity of 2.2, loss tangent of 0.0009, and thickness of 2.54 mm is used. Then, Fig. 8(b) shows that the simulated insertion loss within the operation band is always better than 0.35 dB with the matching capacitive pad. Furthermore, the insertion loss fluctuation over the frequencies is improved by adopting the matching pad. According to Fig. 8(b), the simulated loss variation is less than 0.2 dB within the target operation band.

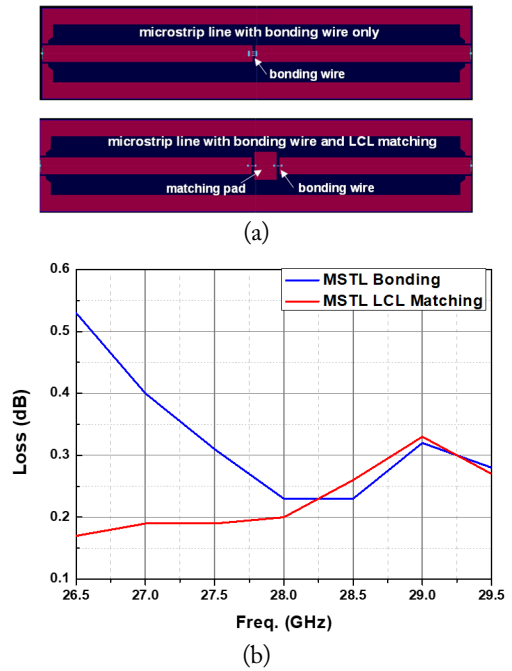


Fig. 8. Analysis of the bonding wire by (a) microstrip transmission line (MSTL) with and without a matching pad, and (b) simulated S -parameters.

III. FABRICATION AND MEASUREMENT

1. Measurement of the Fabricated MMICs

The LNA and PA MMICs are fabricated with the WINsemi 150 nm GaN/SiC process, as shown in Fig. 9(a) and 9(b), respectively. Also, the SPDT switch is fabricated with OMMIC 100 nm GaN/Si process, as shown in Fig. 9(c). The fabricated MMIC sizes of LNA, PA, and SPDT including bonding pads are $3.18 \text{ mm} \times 1.745 \text{ mm}$, $6.15 \text{ mm} \times 2.36 \text{ mm}$, and $1.16 \text{ mm} \times 2.35 \text{ mm}$, respectively. Then, Fig. 10(a) shows the measured S -parameters and NF of the fabricated LNA MMIC in comparison with the simulated results. The measured NF is 2.49 dB at 28 GHz, while the measured NF is always better than 2.52 dB from 26.5 GHz to 29.5 GHz. The measured 10-dB input and output impedance bandwidths are about 14.3% and 17.6%, respectively. Further, the measured gain is always better than 20 dB within the operation band. The measured output P1dB at 26.5 GHz, 28 GHz, and 29.5 GHz are 12 dBm, 12.6 dBm, and 12.6 dBm, respectively. Next, the simulated and measured S -parameters of the fabricated PA MMIC are shown in Fig. 11(a). The measured 10-dB input and output impedance bandwidths are about 8% and 19.6%, respectively, with the center frequency of 28 GHz. The measured gain within the operation band is always better than 15.7 dB, as well. Also, the measured output P1dB at 26.5 GHz, 28 GHz, and 29.5 GHz are 26.6 dBm, 26.6 dBm, and 26.7 dBm, respectively as shown in Fig. 11(b). Furthermore, the measured peak PAE at 26.5 GHz, 28 GHz,

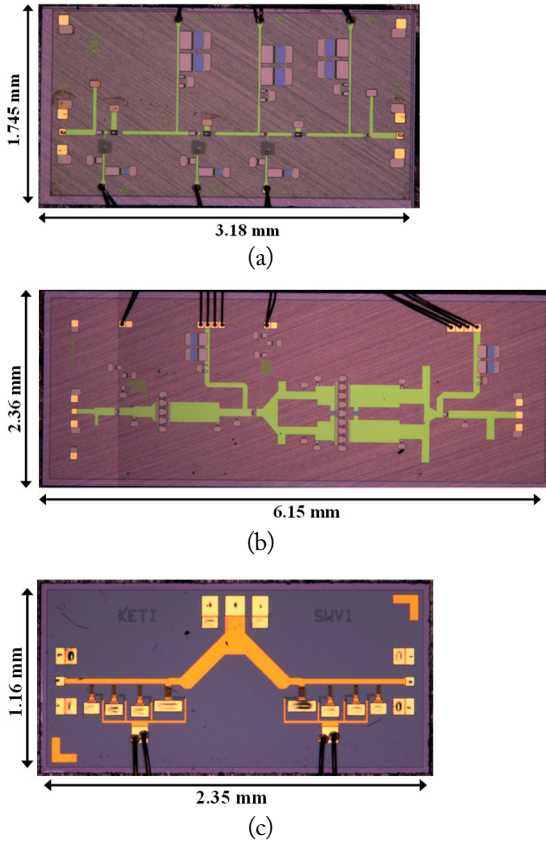


Fig. 9. Fabrication of (a) GaN/SiC LNA, (b) GaN/SiC PA, and (c) GaN/Si SPDT switch MMICs.

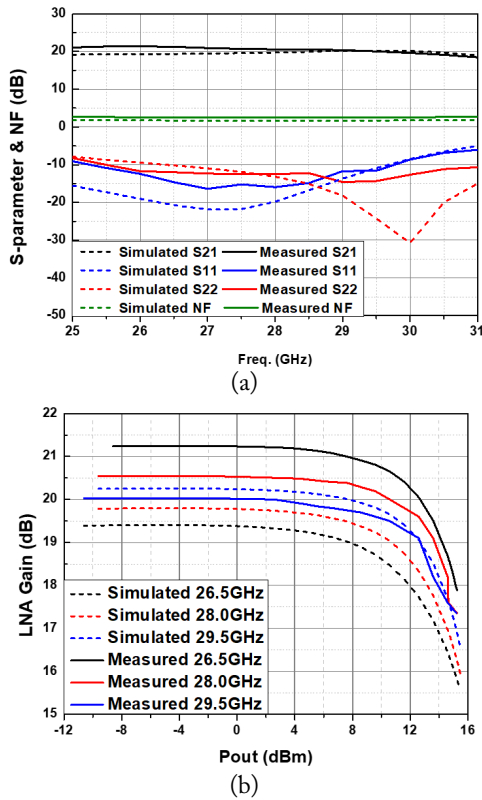


Fig. 10. Simulated and measured (a) S -parameters and NF, and (b) gain and output P1dB of the fabricated GaN/SiC LNA MMIC.

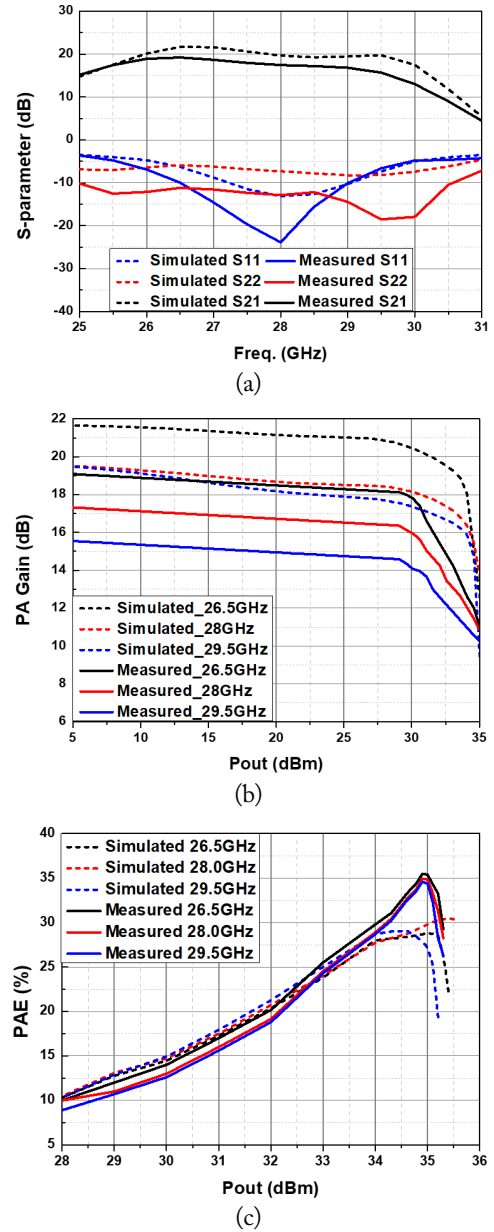
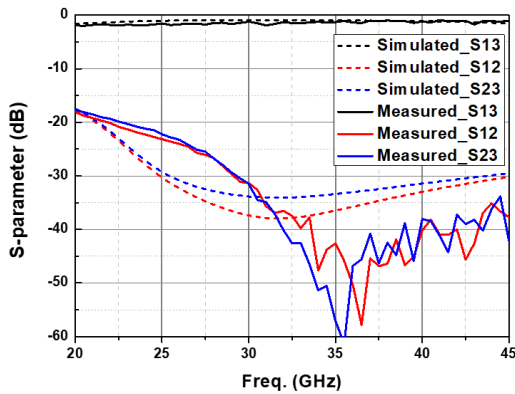
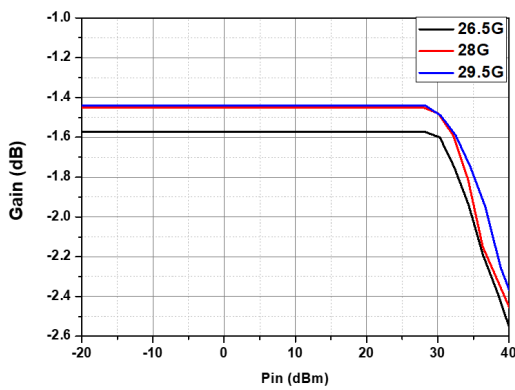


Fig. 11. Simulated and measured (a) S -parameters, (b) output P1dB, and (c) PAE of the fabricated GaN/SiC PA MMIC.

and 29.5 GHz are 35.47%, 34.93%, and 34.58%, respectively as shown in Fig. 11(c). The measured PAE is noted to be unusually higher than the simulated PAE. A mismatch is suspected between the simulation PDK model and real transistor model since we notice a difference between the simulated and measured drain currents. Specifically, the simulated drain currents are 544.7 mA, 545.5 mA, and 543.8 mA, whereas the measured drain currents are 343.2 mA, 349.8 mA, and 354.6 mA at 26.5 GHz, 28 GHz, and 29.5 GHz, respectively for the same output power. Consequently, the measured PAE is found to be higher than the simulated PAE. Finally, Fig. 12 shows the simulated and measured S -parameters of the fabricated SPDT switch MMIC as well as the input P1dB. The 10-dB impedance is



(a)



(b)

Fig. 12. Fabricated GaN/Si SPDT switch MMIC with (a) simulated and measured S -parameters and (b) measured input P1dB.

satisfied over the operation band and the measured insertion loss is always better than 1.92 dB with a variation less than 1 dB. Also, the measured isolation is always better than 24.2 dB within the operation band.

Furthermore, the measured input P1dB is more than 40 dBm, resulting in a sufficient margin for handling PA output power in the target FEM.

2. Implementation and Measurement of the FEM

Before integrating the fabricated GaN MMICs as a single FEM, the conventional transmission lines and the lines with bonding wires are fabricated to verify the interstage line characteristics, as shown in Fig. 13. Each line is fabricated with the TLY-5 substrate identical with the simulation. The microstrip line with the matching pad shows the stable insertion loss within the operation band. The length of the bond wire is 0.35 mm. Further, the dimensions of the matching pad and 50 Ω line are $1.02 \times 1.2 \text{ mm}^2$ and 0.72 mm, respectively. Then, the complete FEM is implemented using the fabricated MMICs and interstage matching lines on a Taconic TLY-5 PCB and a 1.0-mm CPC (Cu-MoCu-Cu) heatsink carrier, as shown in Fig. 14(a). To verify the performance of the complete FEM, both Rx-mode and Tx-mode S -parameters are also measured, as shown

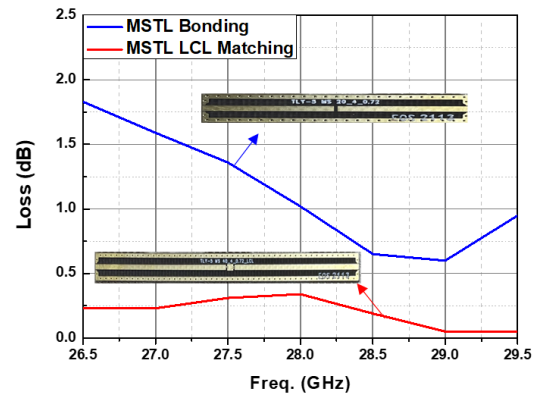
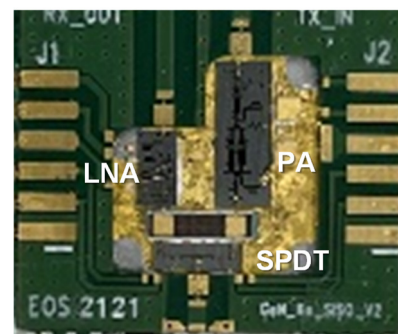
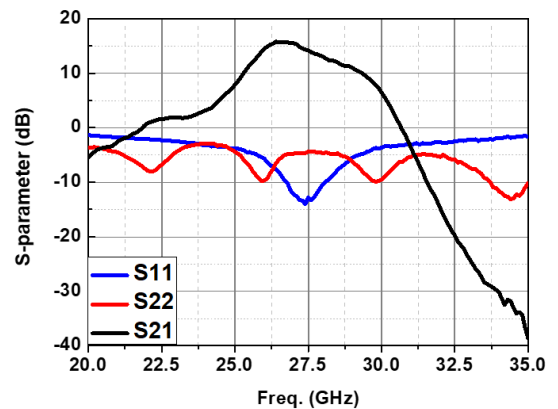


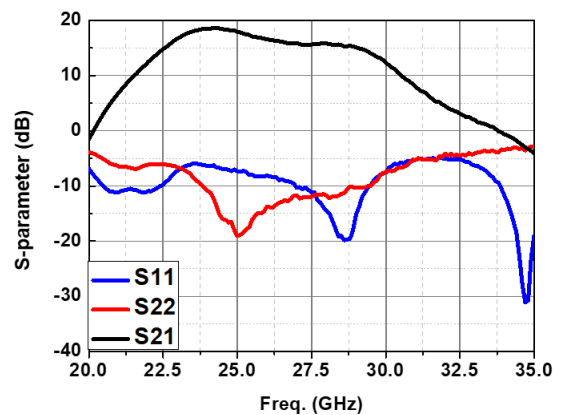
Fig. 13. Measured insertion loss of interstage lines.



(a)



(b)



(c)

Fig. 14. Fabricated FEM with (a) a photograph and measured S -parameters in (b) Rx-mode and (c) Tx-mode.

in Fig. 14(b) and 14(c), respectively. For the Rx mode measurement, 5 V and -1.5 V are applied to VDD and VGS. According to Fig. 14(b), the measured minimum input and output reflection coefficients are about -8.8 dB and -9.9 dB from 26.5 GHz to 29.5 GHz, respectively, in the FEM Rx-mode. The measured small signal gain at 28 GHz is 15.8 dB, while the measured gain variation within the operation band is less than 14 dB. Also, the measured NF within the operation band is always better than 5.47 dB. Next, for the Tx mode measurement, 22.5 V, and -1.5 V and -1.8 V are applied to VDD and each VGS, respectively. The measured minimum input and output reflection coefficients in the FEM Tx-mode are about -4.42 dB and -4.4 dB, respectively, within the operation band, as shown in Fig. 14(c). The measured small signal gain at 28 GHz is 13.07 dB, while the measured gain variation within the operation band is less than 6.4 dB. Finally, the fabricated FEM in the Tx mode is verified with 5G NR 16 QAM and 100 MHz bandwidth test signals as shown in Fig. 15. The measured output powers are 20.18 dBm, 21.03 dBm, and 21.06 dBm, whereas the measured PAEs are 3%, 3.3%, and 2.8% at 26.5 GHz, 28 GHz, and 29.5 GHz, respectively. Furthermore, the measured EVMs are 4.65%, 4.78%, and 4.14% at 26.5 GHz, 28 GHz, and 29.5 GHz, respectively.

IV. CONCLUSION

In this paper, the mmWave-5G FEM configured by GaN/SiC LNA and PA MMICs, as well as a GaN/Si SPDT switch MMIC, is presented. Each MMIC is fabricated individually

and shows a good agreement between the simulation and measurement. Then, all MMICs are integrated within a single carrier as an FEM and successfully verified by a 5G NR signal with 16-QAM, 100 MHz bandwidth, and 120 kHz source carrier spacing.

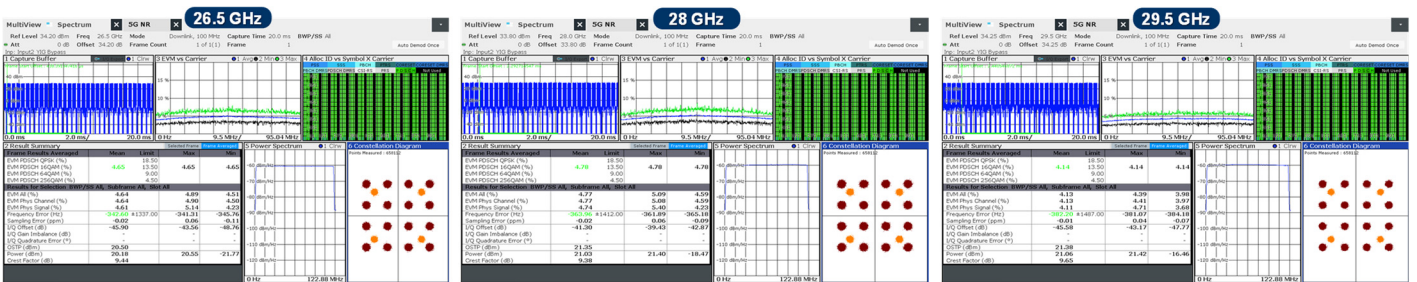
This work was supported in part by the Development of Civil Military Technology program (No. 21-CM-RA-02) from the Institute of Civil Military Technology Cooperation (ICMTC), and in part by the Korea Institute for Advancement of Technology (KIAT) grant funded by the Korea government (MOTIE) (No. P0017011, HRD Program for Industrial Innovation), and in part by the Chung-Ang University Research Scholarship Grants in 2020.

REFERENCES

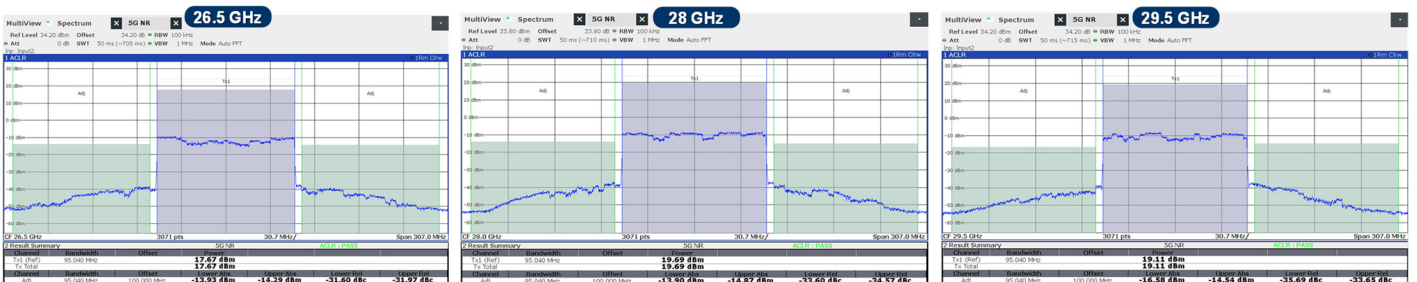
[1] D. P. Nguyen, B. L. Pham, and A. V. Pham, "A compact Ka-band integrated Doherty amplifier with reconfigurable input network," *IEEE Transactions on Microwave Theory and Techniques*, vol. 67, no. 1, pp. 205-215, 2019.

[2] A. Inoue, "Millimeter-wave GaN devices for 5G: massive MIMO antenna arrays for sub-6-GHz and mm-wave bandwidth," *IEEE Microwave Magazine*, vol. 22, no. 5, pp. 100-110, 2021.

[3] G. Lv, W. Chen, X. Liu, and Z. Feng, "A dual-band GaN MMIC power amplifier with hybrid operating modes for 5G application," *IEEE Microwave and Wireless Components*



(a)



(b)

Fig. 15. A 5G NR test with the proposed FEM Tx: (a) EVM test and (b) ACPR test.

- Letters*, vol. 29, no. 3, pp. 228-230, 2019.
- [4] V. Camarchia, R. Quaglia, A. Piacibello, D. P. Nguyen, H. Wang, and A. V. Pham, "A review of technologies and design techniques of millimeter-wave power amplifiers," *IEEE Transactions on Microwave Theory and Techniques*, vol. 68, no. 7, pp. 2957-2983, 2020.
- [5] H. Tao, J. Wang, Y. Wang, D. Ma, H. Cao, W. Wu, and T. Huang, "High-power Ka/Ku dual-wideband GaN power amplifier with high input isolation and transformer-combined load design," *IEEE Microwave and Wireless Components Letters*, vol. 31, no. 1, pp. 49-51, 2021.
- [6] R. Giofre, S. Colangeli, W. Ciccognani, F. Costanzo, G. Polli, A. Salvucci, et al., "S-band GaN single-chip front end for active electronically scanned array with 40-W output power and 1.75-dB noise figure," *IEEE Transactions on Microwave Theory and Techniques*, vol. 66, no. 12, pp. 5696-5707, 2018.
- [7] R. Giofre, F. Costanzo, W. Ciccognani, S. Colangeli, and E. Limiti, "GaN single-chip front end with improved efficiency and power by using class F approach," *IEEE Microwave and Wireless Components Letters*, vol. 29, no. 2, pp. 140-142, 2019.
- [8] M. van Heijningen, P. de Hek, C. Dourlens, P. Fellon, G. Adamiuk, N. Ayllon, and F. van Vliet, "C-band single-chip radar front-end in AlGaIn/GaN technology," *IEEE Transactions on Microwave Theory and Techniques*, vol. 65, no. 11, pp. 4428-4437, 2017.
- [9] M. Thorsell, M. Fagerlind, K. Andersson, N. Billstrom, and N. Rorsman, N. (2009). "An X-band AlGaIn/GaN MMIC receiver front-end," *IEEE Microwave and Wireless Components Letters*, vol. 20, no. 1, pp. 55-57, 2010.
- [10] Q. Lin, H. Wu, Y. Chen, L. Hu, S. Chen, and X. Zhang, "A compact ultra-broadband GaN MMIC T/R front-end module," in *Proceedings of 2020 IEEE/MTT-S International Microwave Symposium (IMS)*, Los Angeles, CA, 2020, pp. 1231-1234.

Ji-Hye Hwang



received the B.S. degree in electronics engineering from Hansoo University, Seosan, South Korea, in 2018, and the M.S. degree in electronics and electrical engineering from Chung-Ang University, Seoul, South Korea, in 2021, respectively. Since 2017, she has been a research engineer in ICT Device & Packaging research center at Korea Electronics Technology Institute. Her research interests include RF circuits and communication systems, power amplifier module (PAM), RFIC/MMIC, and front-end module (FEM).

Ki-Jin Kim



received the B.S. degree in electrical engineering from Kookmin University, Seoul, South Korea, in 2003 and M.S. and Ph.D. degrees in electrical engineering from KAIST, Daejeon, South Korea, in 2006, 2013, respectively. From 2006 to 2018, he was a senior researcher and now he is a team leader in ICT device packaging center at Korea Electronics Technology Institute (KETI). His research interests include CMOS RF circuits, compound semiconductor MMIC, and modeling of the RF transistors.

Jiho Lee



received the B.S. degree from Korea Aerospace University (KAU), Goyang, South Korea, in 2020. He is currently pursuing the M.S. degree in electrical and electronics engineering at Chung-Ang University, Seoul, South Korea. His research interests include mm-Wave antennas, and RF circuits.

Han Lim Lee



received the B.A.Sc. degree in electronics engineering from Simon Fraser University, BC, Canada, in 2008 and the M.S. and Ph.D. degrees in electrical engineering from KAIST, Daejeon, South Korea, in 2010, and 2014, respectively. From 2014 to 2015, he was a senior engineer in DMC research center at Samsung Electronics. In 2015, he joined the school of electrical and electronics engineering in Chung-Ang University, where he is currently an associate professor. His research interests include RF circuits and communication systems, mmWave beam-forming antennas and phased array systems, antenna-in-package, RFIC/MMIC, scalable-RF module, and microwave wireless power transmission (MWPT).